Synthesis and Evaluation of Silanediols as Highly Selective Uncompetitive Inhibitors of Human Neutrophil Elastase

Julie L. H. Madsen,[†] Thomas L. Andersen,[†] Salvatore Santamaria,[‡,§] Hideaki Nagase,[‡,§] Jan J. Enghild,*,[∥] and Troels Skrydstrup*,[†]

[†]Center for Insoluble Protein Structures, Department of Chemistry, and Interdisciplinary Nanoscience Center, Aarhus University, Langelandsgade 140, 8000 Aarhus C, Denmark

[‡]Faculty of Medicine, Imperial College London, 65 Aspenlea Road, London W6 8LH, U.K.

[§]The Kennedy Institute of Rheumatology, Nuffield Department of Orthopaedics, Rheumatology and Musculoskeletal Sciences, University of Oxford, 65 Aspenlea Road, London W6 8LH, U.K.

[∥]Center for Insoluble Protein Structures, Department of Molecular Biology and Genetics, and Interdisciplinary Nanoscience Center, Aarhus University, Gustav Wieds Vej 10, 8000 Aarhus C, Denmark

S *Supporting Information*

ABSTRACT: Chronic obstructive pulmonary disease (COPD) is an increasing health problem and is estimated to be the fifth leading cause of death in 2020 according to the World Health Organization. Current treatments are only palliative, and therefore the development of new medicine for the treatment of COPD is urgent. Human Neutrophil Elastase (HNE) is a serine protease that is heavily involved in the progression of COPD through inflammatory breakdown of lung tissue. Consequently, inhibitors of HNE are of great

interest as therapeutics. In this article, the development of silanediol peptide isosters as inhibitors of HNE is presented. Kinetic studies revealed that incorporation of a silanediol isoster in the inhibitor structure resulted in an uncompetitive mechanism of inhibition, which further resulted in excellent selectivity. The peculiar mechanism of inhibition and the resulting selectivity makes the presented inhibitors promising leads for the development of new HNE-inhibitor-based therapeutics for the treatment of COPD.
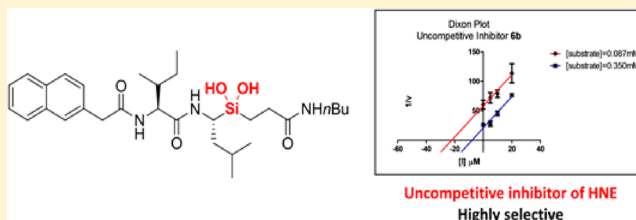
INTRODUCTION

Human Neutrophil Elastase (HNE) is a serine protease belonging to the chymotrypsin family. The enzyme is stored in the azurophilic granules of neutrophils where it participates in the degradation of engulfed pathogens. HNE efficiently degrades elastin and other extracellular matrix proteins, and upon inflammation, HNE is released by neutrophils and assists in neutrophil migration to the site of inflammation.[1−3] In order to prevent an excessive breakdown of healthy tissue at physiological conditions, the activity of extracellular HNE is controlled by endogenous serine protease inhibitors (SERPINs) like the α1-protease inhibitor (α1-PI). An imbalance between levels of extracellular HNE and the endogenous SERPINs leads to various pathological conditions, such as chronic obstructive pulmonary diseases (COPD),[4] acute respiratory distress syndrome,[5] acute lung injury,[6] and cystic fibrosis.[7] Such imbalances can result either from inherited mutations of the SERPIN or from SERPIN oxidation by cigarette smoke, both resulting in inactivation of the SERPIN. Animal studies have revealed that a reduced level of catalytically active HNE, either by genetic deficiency or inhibition of HNE, protects against pro-inflammatory effects of chronic cigarette smoke exposure.[8,9] Therefore, the identification of selective

inhibitors of HNE could show great potential as therapeutics for the various pathological conditions arising from the role of HNE in the inflammatory process and lung tissue damage.

The increased focus on the development of HNE inhibitor-based therapeutics has, during the past two decades, resulted in numerous HNE inhibitors reported in the literature, some of which have undergone clinical trials.[10,11] The small molecule inhibitors published have, to the best of our knowledge, all been active site-directed competitive inhibitors, and a common structural inhibitor motif is based on a Val-Pro-Val tripeptide part binding to the active site cleft combined with a *C*-terminal electrophilic carbonyl interacting with the catalytic serine residue (Figure 1, inhibitor **1**).[12] In addition, many heterocyclic and acetylating inhibitors have been developed (Figure 1, inhibitors **2** and **3**).[13,14] Despite the numerous inhibitors published, so far only one compound has entered the market (Figure 1, inhibitor **2**). This is an acetylating inhibitor and is applied for the treatment of acute lung injury (ALI) in Japan, whereas the clinical trials in the western world were abandoned in 2003.[15] The majority of HNE inhibitors have failed clinical
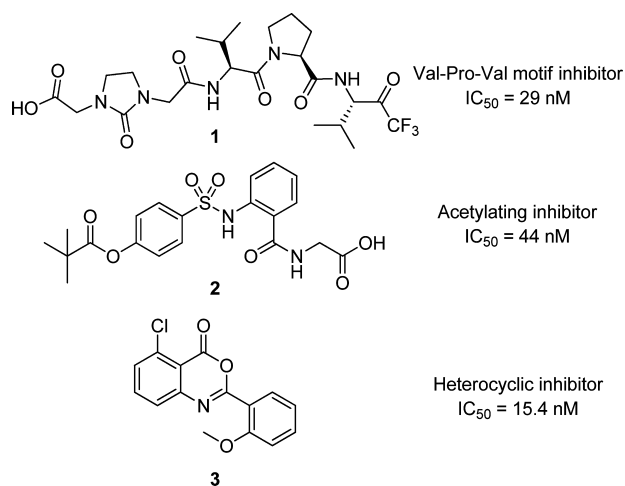
Figure 1. Examples of three types of previously reported HNE inhibitors.

trials due to a lack in proof of therapeutic effect or due to toxicity resulting from a lack of selectivity.[16]

In general, proteases represent a significant therapeutic target due to their essential physiological roles. Often a transition state isoster motif is applied in the design of new inhibitors. Silanediols are one example of such isosters that mimic the tetrahedral intermediate of protein hydrolysis due to the inherent stability of the geminal diol as compared to their carbon analogue. Examples of silanediols as inhibitors of aspartic- and metalloproteases have been reported by Sieburth et al. (Figure 2, inhibitors **4** and **5**).[17,18] Silanediol **4** is an
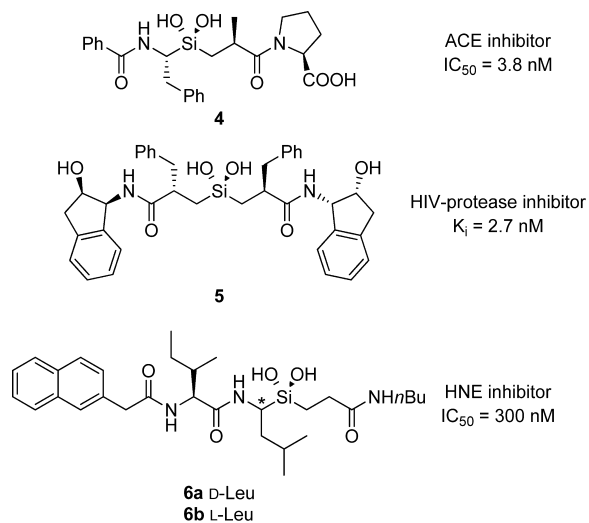

**Figure 2.** Examples of silanediol-based protease inhibitors.

inhibitor of angiotensin-converting enzyme with an IC$_{50}$ of 3.8 nM, whereas, silanediol **5** inhibits the HIV protease with a K_i value of 2.7 nM. Compounds **6a** and **6b** were published in 2004 as a potent inhibitor of HNE.[19,20] The silanediols were synthesized and evaluated as a mixture of epimers and showed an IC$_{50}$ of 300 nM. The inhibitor was designed *in silico* to fit the active site binding pocket; however, an experimental study of the mechanism of inhibition has not been reported. To our knowledge, this is the first example of a silanediol acting as a serine protease inhibitor, and we therefore became interested in studying the mechanism of inhibition of this compound.

In this article, we report the stereoselective synthesis of compound **6b** and analogues hereof, and show that such compounds containing the silanediol moiety display an uncompetitive mechanism of inhibition which proved important for selectivity over six other serine proteases in this study, some of which are closely related to HNE.

RESULTS AND DISCUSSION

Chemistry and Design. A stereoselective synthesis of enantiomerically pure silanediol **6b** was easily achieved by applying a method previously developed by our group; addition of a silyllithium reagent to an Ellman chiral sulfinimine was the key step of the synthesis pathway and fully controlled the stereochemistry at the α-carbon at the N-terminal side of the silanediol (Scheme 1).[21,22] Synthesis of compound **6b** was

Scheme 1. Synthetic Strategy for the Stereoselective Synthesis of Inhibitor 6b
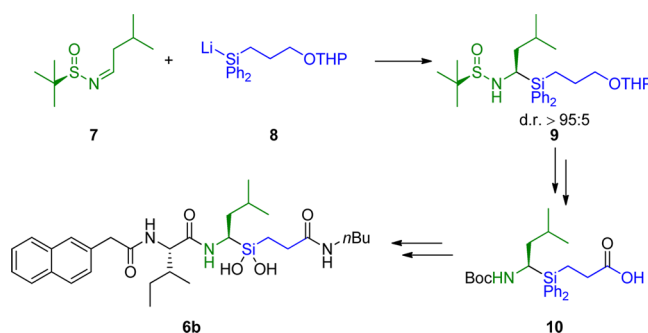
chosen over **6a** due to the natural L-amino acid configuration of the leucine residue in **6b**. Preliminary enzyme kinetics experiments revealed that inhibitor **6b** did not compete with the chromogenic substrate and was therefore not a competitive inhibitor of HNE. This finding is in contrast to the previously published *in silico* design of silanediols **6a** and **6b** binding to the active site as a competitive inhibitors of HNE.[20] In order to further investigate the mechanism of inhibition and structure–activity relationship (SAR) of these types of compounds, a small library of 11 inhibitors was developed.

Since inhibitor **6b** was not competitive, the binding pocket at HNE was unknown. The library was therefore kept simple with the design of the analogues based on the already published inhibitor **6b**. Simple variations were made on the N- and C-terminal capping groups, the substituents on silicon, and in addition, regular peptides were included in the library in order to determine the importance of the silanediol isoster for the inhibition (Figure 3).

Silanediol inhibitors **6b** and **11–14** were synthesized by following the previously published procedure, and diphenylsilane **16** is the precursor of inhibitor **6b** (Scheme 2).[23] Hydrosilylation of 2-(allyloxy)-tetrahydro-2H-pyran afforded diphenylsilane **22**, which upon lithiation and addition to sulfinimine **7** afforded the diphenylsilane analogue of L-leucine **9**. Protecting group manipulations and oxidation of the primary alcohol provided dipeptide fragment **10**, and standard solution phase peptide synthesis was applied for reactions with the C-terminal capping group, isoleucine, and the N-terminal capping group. A final deprotection of the diphenylsilanes **16** and **26**–**29** was achieved by using trifluoromethanesulfonic acid, and the difluorosilanes **6b′** and **11′**–**14′** were isolated following treatment with aqueous hydrofluoric acid.
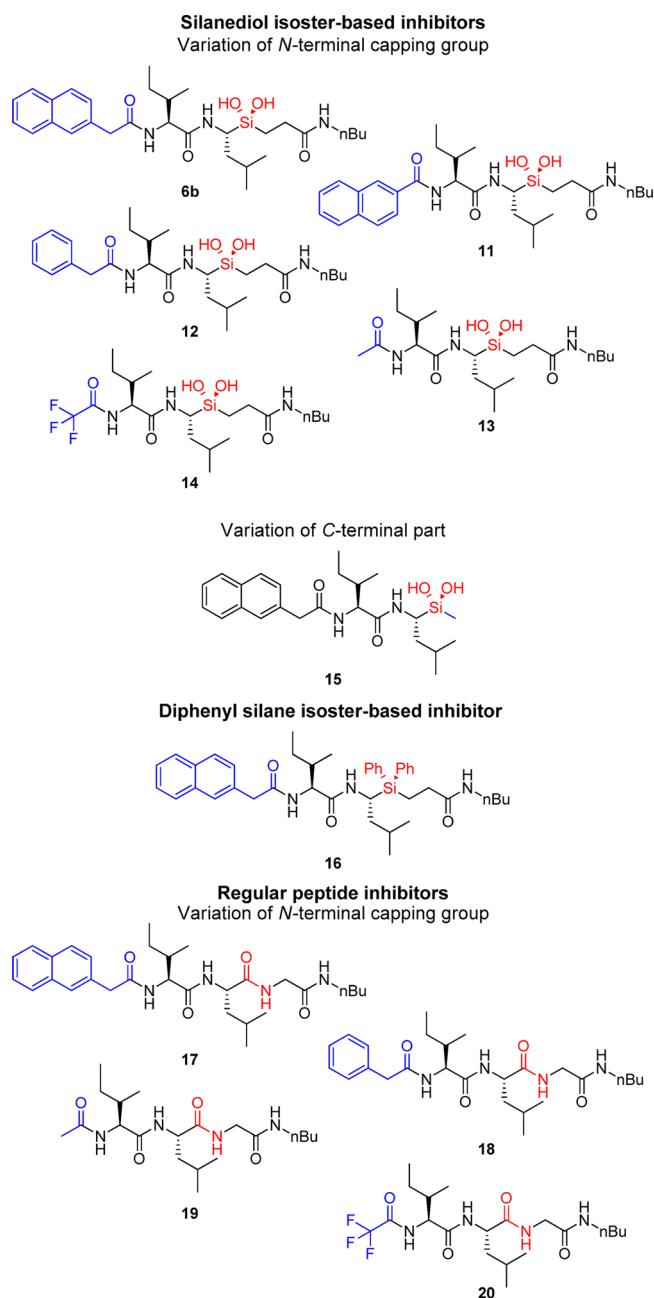
Figure 3. Inhibitor analogues included in the SAR study.

Silanediol inhibitor **15** was prepared via a di-*p*-tolylsilane route (Scheme 3). Treatment of dichloromethylsilane with *p*-tolyl-grignard reagent afforded di-*p*-tolylsilane **31**. Lithiation and addition to sulfinimine **7** followed by protecting group manipulations afforded the di-*p*-tolylsilane analogue of L-leucine **33**. Again, standard solution phase peptide synthesis was applied for the elongation of the peptide backbone. Di-*p*-tolylsilane **35** was converted into the silanediol by applying a method, previously published by our group, which uses milder cleavage conditions;[24] the di-*p*-tolylsilane deprotection was achieved by using a 1:1 solution of tifluoroacetic acid and CH2Cl2. Difluorosilane **15′** was isolated after treatment with aqueous hydrofluoric acid.

The regular peptide inhibitors **17–20** were synthesized by solution phase peptide synthesis using a standard Boc-protection strategy (Scheme 4).

Because of the low stability of isolated silanediols, inhibitors **6b** and **11–15** were isolated as the difluorosilanes **6b′** and **11′–15′** as can be seen from Schemes 2 and 3. However, upon solvation in assay buffer, the fluorides are exchanged for hydroxyl groups, affording the desired silanediols. This was confirmed by NMR studies of **6b′** in assay buffer revealing that the fluoride signals from the difluorosilane disappeared, and a signal at −119 appeared, corresponding to sodium fluoride.[25] The inhibitory data are therefore presented for the silanediols as these are the active species at the applied assay conditions.

Biology. The inhibitory potency of the 11 analogues against human neutrophil elastase (HNE) was tested *in vitro* using the chromogenic substrate *N*-succinyl-Ala-Ala-Pro-Val-*p*-nitroani-lide. The resulting IC_{50} values are reported in Table 1.

As can be seen from the data here reported, the presence of an aromatic *N*-terminal capping group proved important for inhibition. Inhibitors, **6b**, **11**, **16**, and **17** containing an *N*-terminal naphthyl substituent all displayed IC_{50} values in the range of 14–18 μM, whereas inhibitors **13**, **14**, **19**, and **20** containing *N*-terminal acetyl or trifluoroacetyl groups exhibited low or no inhibition. The *C*-terminal part of the inhibitor did not prove vital for inhibition; however, an increase in IC_{50} was observed upon its removal, as observed with inhibitor **15**. When evaluating the importance of the isoster, it was seen by comparing inhibitor **6b**, **16**, and **17** that the silanediol, the diphenylsilane, and the regular peptide all show inhibitory potency in the same range. These data indicate that the silanediol isoster moiety is not important for the inhibition of HNE. This is in good agreement with the preliminary results demonstrating that inhibitor **6b** does not interact with the active site catalytic serine residue and does therefore not act as a regular transition state inhibitor. In the case of silanediol-based transition state inhibitors of metallo- and aspartyl proteases, the silanediol mimics the tetrahedral intermediate of hydrolysis accurately, with H2O acting as nucleophile in the proteolysis (Figure 4a). However, with the serine proteases, a serine residue plays the role of nucleophile during hydrolysis, thereby forming a covalently bound intermediate to the enzyme (Figure 4b). Hence, silanediols are not obvious transition state inhibitors for the competitive inhibition of serine proteases, which is again in good agreement with the results obtained.

From the data obtained on the inhibitory potency, the five best compounds, inhibitors, **6b**, **11**, **12**, **16**, and **17**, were chosen for further studies on the mechanism of inhibition. The inhibition of HNE was measured at two different substrate concentrations and Dixon plots and Cornish−Bowden plots were prepared.[26,27] Representative plots are shown in Figure 5.

The results showed a clear trend on the mechanism of inhibition, depending on the type of inhibitor. Inhibitors **6b**, **11**, and **12**, containing the silanediol moiety, followed an uncompetitive mechanism of inhibition. This was seen from the parallel curves in the Dixon plot and the intercept above the *x*-axis in the Cornish−Bowden plot (Figure 5a). The K_i value was obtained from the negative *x*-value of the intercept in the Cornish−Bowden plots (Table 1). In contrast, the diphenylsilane **16** and the regular peptide inhibitor **17** displayed a noncompetitive mechanism of inhibition, as was seen from the intercept at the *x*-axis in the Dixon plot and below the *x*-axis in the Cornish−Bowden plot (Figure 5b). For inhibitors **16** and **17** the K_i value was obtained from the negative *x*-value of the intercept at the *x*-axis in the Dixon plot. Interestingly, this difference in mechanism did not prove important for the inhibitory potency as was seen from the similar IC_{50} values of

Scheme 2. Synthesis of Silanediol-Based Inhibitor Analogues[a]
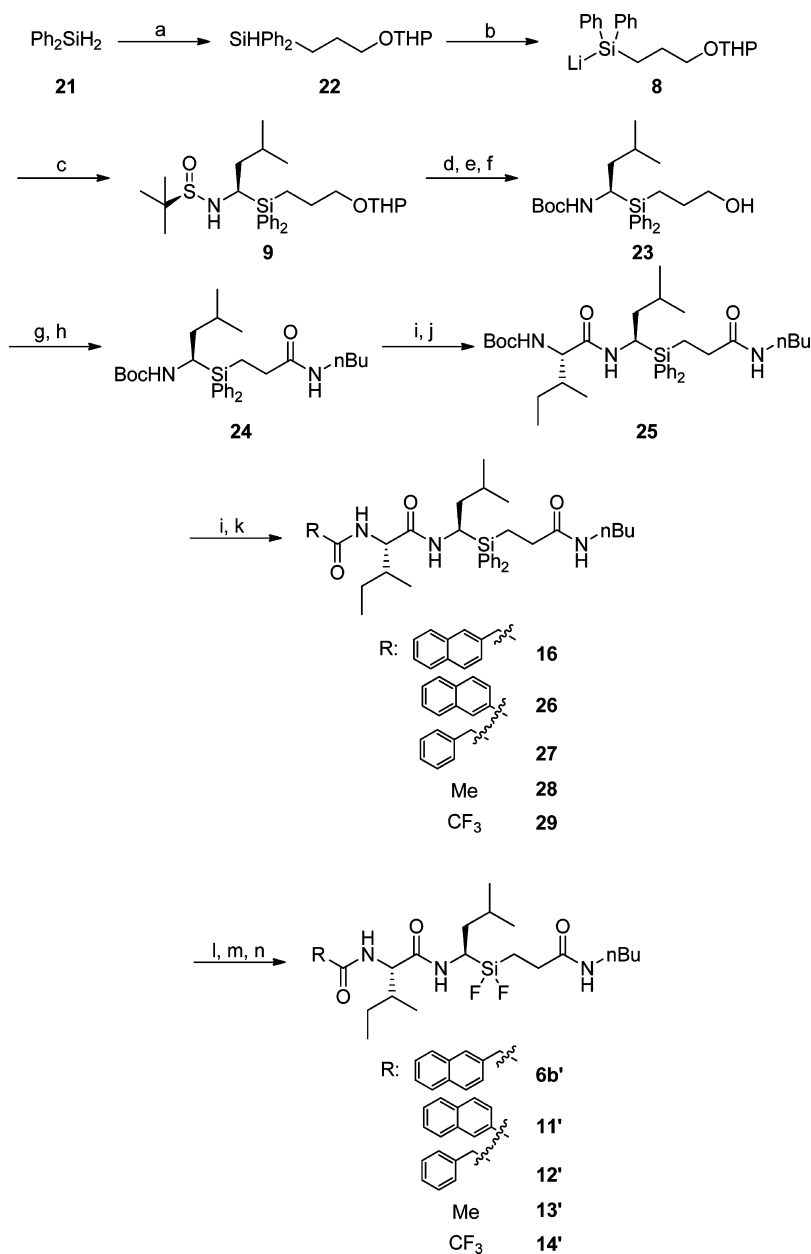
[a]Reagents: (a) 2-(Allyloxy)tetrahydro-2H-pyran, chlorotris(triphenylphosphino)-rhodium(I), THF; (b) lithium(s), THF; (c) (R,E)-2-methyl-N-(3-methylbutylidene)propane-2-sulfinamide, THF; (d) HCl in MeOH (0.5M); (e) di-tert-butyl dicarbonate, triethylamine, CH$_2$Cl$_2$; (f) NaOH (2M), CH$_2$Cl$_2$; (g) sodium (meta)periodate, ruthenium(III) chloride, acetonitrile, water, ethyl acetate; (h) n-butylamine, 1-(3-dimethylaminopropyl)-3-ethylcarbodiimide, 1-hydroxy-benzotriazole, N-methyl morpholine, CH$_2$Cl$_2$; (i) trifluoroacetic acid, CH$_2$Cl$_2$; (j) N-(tert-Butoxycarbonyl)-L-isoleucine, hemihydrate, 1-(3-dimethylaminopropyl)-3-ethylcarbodiimide, 1-hydroxybenzotriazole, N-methyl morpholine, CH$_2$Cl$_2$; (k) corresponding carboxylic acid, 1-(3-dimethylaminopropyl)-3-ethylcarbodiimide, 1-hydroxybenzotriazole, N-methyl morpholine, CH$_2$Cl$_2$; (l) trifluoromethanesulfonic acid, CH$_2$Cl$_2$; (m) ammonium hydroxide (28%), CH$_2$Cl$_2$; (n) hydrofluoric acid (48% aqueous solution), CH$_2$Cl$_2$.

the five inhibitors. However, these interesting mechanisms of inhibition prompted us to expect better selectivities of these inhibitors as compared to the numerous competitive HNE inhibitors reported in the literature and clinical trials. Since serine proteases are rather similar, with the active site built around the catalytic triad of serine, histidine, and aspartate, competitive inhibitors, which interact with the catalytic serine residue, might also easily interact with catalytic serine residues of other serine proteases, resulting in low selectivity and therefore high toxicity when administered as a drug. The observation that the inhibitors presented in this work follow

un- or noncompetitive mechanisms might result in more selective inhibitors and provide a new route for the development of HNE-inhibitor-based therapeutics for the treatment of the various lung-tissue-damaging diseases.

In order to test the hypothesis of the uncompetitive and noncompetitive inhibitors exhibiting improved selectivities, the inhibitors, **6b**, **11**, **12**, **16**, and **17**, were tested in vitro in chromogenic assays for the inhibitory potency of six other serine proteases, including, plasmin, thrombin, cathepsin G, porcine pancreatic elastase (PPE), trypsin, and chymotrypsin, some of which have up to 40% homology with HNE. The

Scheme 3. Synthesis of Silanediol 15 via Di-*p*-tolylsilane[*a*]
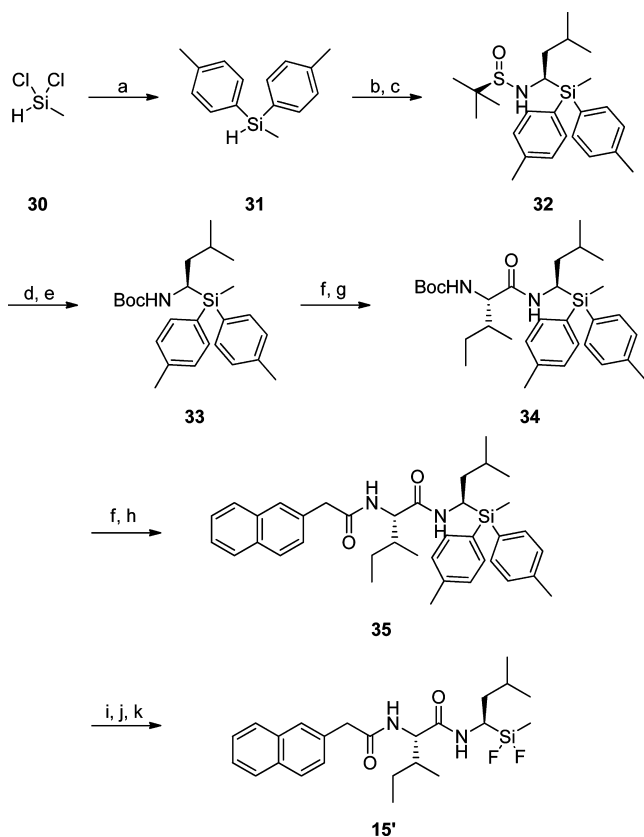
[*a*]Reagents: (a) *p*-bromotoluene, Mg-bands, dibromoethane, THF; (b) Li(s), THF; (c) (*R,E*)-2-methyl-*N*-(3-methylbutylidene)propane-2-sulfinamide, THF; (d) HCl in MeOH (0.5M); (e) di-*tert*-butyl dicarbonate, triethylamine, CH₂Cl₂; (f) trifluoroacetic acid, CH₂Cl₂; (g) *N*-(*tert*-butoxycarbonyl)-L-isoleucine, hemihydrate, 1-(3-dimethylaminopropyl)-3-ethylcarbodiimide, 1-hydroxybenzotriazole, *N*-methyl morpholine, CH₂Cl₂; (h) 2-naphthaleneacetic acid, 1-(3-dimethylaminopropyl)-3-ethylcarbodiimide, 1-hydroxybenzotriazole, *N*-methyl morpholine, CH₂Cl₂; (i) trifluoroacetic acid, CH₂Cl₂; (j) ammonium hydroxide (28%), CH₂Cl₂; (k) hydrofluoric acid (48% aqueous solution), CH₂Cl₂.

results are presented in Table 2. For the selectivity data, a clear trend was observed. Inhibitors **6b**, **11**, and **12**, which followed an uncompetitive mechanism of inhibition of HNE, did not display inhibition of any of the six serine proteases up to the maximum assay concentration (100 μM), whereas the two noncompetitive inhibitors, **16** and **17**, both revealed varied inhibition of the six enzymes. A general irreversible serine protease inhibitor, 4-(2-aminoethyl) benzenesulfonyl fluoride hydrochloride (AEBSF), was also included in the tests as a positive control for inhibition, and the IC₅₀ values were determined for all seven enzymes in this study (Table 2). The trend of the selectivity data complements the determined mechanisms of inhibition and suggests that an uncompetitive inhibitor does supply a better selectivity than the noncompetitive inhibitors. Interestingly, this suggests that the silanediol moiety, although not affording better inhibitory potency, is important for providing an uncompetitive mechanism of inhibition and thereby yielding highly selective inhibitors of HNE.

CONCLUSIONS

Overall, this study has provided important information on the SAR and mechanism of the presented silanediol-type inhibitors for the inhibition of HNE. A highly interesting uncompetitive mechanism of inhibition was observed for inhibitors, **6b**, **11**, and **12**, resulting in excellent selectivity over six other serine proteases. The presented inhibitors therefore represent a promising avenue to pursue for the development of important therapeutics for the treatment of COPD and related diseases.

In future studies, the mode of HNE binding will be investigated in a combined study exploiting hydrogen exchange mass spectrometry (HXMS) and MD-simulations. This knowledge will be of high importance for further development of interesting potent and selective inhibitors of HNE.

EXPERIMENTAL PROCEDURES

Chemistry. Solvents were dried according to standard procedures. All commercially available reagents were used as received without further purification unless otherwise noted. All reactions were performed under inert atmosphere unless otherwise noted. Reactions were monitored by thin-layer chromatography (TLC) analysis. Flash chromatography was performed using silica gel 60 (230−400 mesh). ¹H NMR was recorded at 400 MHz, ¹³C NMR at 100 MHz and ¹⁹F NMR at 377 MHz. The chemical shifts are reported in ppm relative to solvent residual peak.[28] Multiplicities are reported using the following abbreviations: s = singlet, bs = broad singlet, d = dublet, t = triplet, q = quartet, quin = quintet, hex = hextet, hep = heptet, non = nonet, and m = multiplet. HRMS was recorded on a TOF-MS (ESI) apparatus.

The purity of all tested inhibitor analogues were confirmed as ≥95% using analytical RP-HPLC performed using an Agilent 1100 system with a KINETEX column (C18, 4.6 mm × 150 mm, 2.6 μm, 100 Å) operated at a flow rate of 1 mL/min at 25 °C and a linear gradient from 5 to 90% B in A. The solvent systems applied were A (0.1% trifluoroacetic acid in H₂O) and B (0.1% trifluoroacetic acid in acetonitrile). Absorbance was monitored at 215 nm and product purities measured as peak area percentage at 215 nm.

General Procedure A: TFA-Mediated Boc Deprotection and EDC Coupling. To a solution of carbamate (0.2 mmol) in CH₂Cl₂ (2.5 mL) was added trifluoroacetic acid (1.25 mL), and the reaction was stirred for 2 h. All volatiles were removed *in vacuo*, and the crude compound was washed three times by addition and evaporation of CH₂Cl₂. The TFA-salt of the deprotected peptide (0.2 mmol) was dissolved in CH₂Cl₂ (2.5 mL) and then *N*-methylmorpholine (0.8 mmol), carboxylic acid (0.4 mmol), HOBt (0.8 mmol), and EDC (0.4 mmol) were added, and the reaction was stirred for 24 h. The reaction mixture was poured into water and extracted with CH₂Cl₂. The combined organic phases were dried over MgSO₄, filtered, and evaporated *in vacuo*. Pure product was obtained by flash chromatography (FC).

General Procedure B: Diphenylsilane Deprotection. To a solution of diphenylsilane (0.030 mmol) in CH₂Cl₂ (2 mL) at 0 °C was dropwise added triflic acid (0.450 mmol), and the reaction was stirred overnight while allowed to warm to rt. The reaction was cooled to 0 °C and ammonium hydroxide (25%w/w, 0.785 mmol) was added. The reaction was stirred for 1 h at 0 °C after which hydrofluoric acid (48% in H₂O, 2.260 mmol) was added, and the reaction was stirred for further 30 min. CH₂Cl₂ was added, and the reaction was washed with H₂O and brine, dried over Na₂SO₄, and evaporated *in vacuo*, affording the product.

(2S,3S)-*N*-((*R*)-1-((3-(Butylamino)-3-oxopropyl)difluo-rosilyl)-3-methylbutyl)-3-methyl-2-(2-(naphthalen-2-yl)acetamido)-pentanamide (6b'). The compound was synthesized according to a literature procedure.[23] ¹H NMR (400 MHz, CDCl₃) δ (ppm) 3.78−3.85 (m, 4H), 7.75 (s, 1H), 7.45−7.51 (m, 2H), 7.37 (dd, 1H, *J* = 8.4 Hz, *J* = 1.7 Hz), 6.52 (d, 1H, *J* = 8.8 Hz), 5.64 (bs, 1H), 4.45 (t, 1H, *J* = 8.4 Hz), 3.76 (dd, 2H, *J* = 19.4 Hz, *J* = 15.4 Hz), 3.18−3.25 (m, 2H), 2.74−2.81 (m, 1H), 2.19−2.32 (m, 2H), 1.73−1.83 (m, 1H), 1.54−1.65 (m, 1H), 1.23−1.54 (m, 8H), 0.94−1.05 (m, 2H), 0.76−

Scheme 4. Synthesis of Regular Peptide Inhibitors[a]
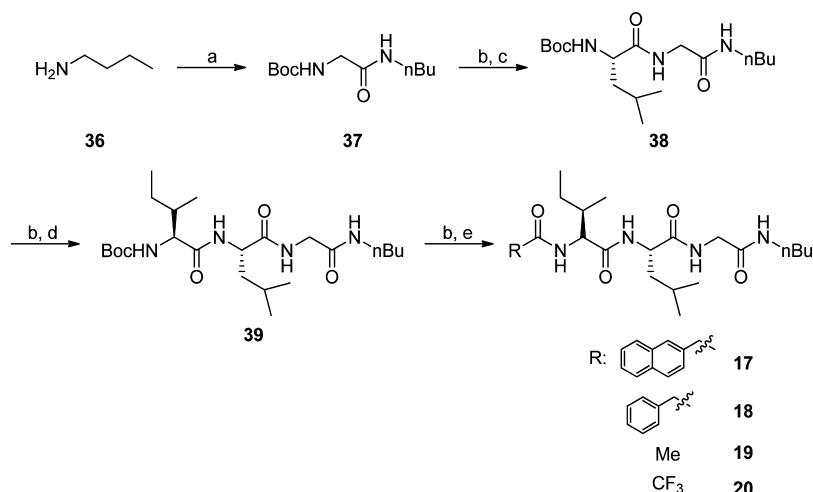
[a]Reagents: (a) N-(tert-butoxycarbonyl)glycine, 1-(3-dimethylaminopropyl)-3-ethylcarbodiimide, 1-hydroxybenzotriazole, N-methyl morpholine, CH₂Cl₂; (b) trifluoroacetic acid, CH₂Cl₂; (c) N-(tert-butyloxycarbonyl)-L-leucine, 1-(3-dimethylaminopropyl)-3-ethylcarbodiimide, 1-hydroxybenzotriazole, N-methyl morpholine, CH₂Cl₂; (d) N-(tert-Butoxycarbonyl)-L-isoleucine, hemihydrate, 1-(3-dimethylaminopropyl)-3-ethylcarbodiimide, 1-hydroxybenzotriazole, N-methyl morpholine, CH₂Cl₂; (e) corresponding carboxylic acid, 1-(3-dimethylaminopropyl)-3-ethylcarbodiimide, 1-hydroxybenzotriazole, N-methyl morpholine, CH₂Cl₂.

Table 1. Kinetic Data[a] **for HNE Inhibition**

inhibitor	IC$_{50}$ (μM)	K_i (μM)
6b	18	3.5
11	16	4.0
12	38	5.0
13	>200	
14	46	
15	39	
16	14	13.0
17	14	18.0
18	51	
19	>200	
20	>200	

[a]The IC$_{50}$ and K_i values are the average of at least two determinations with a standard deviation of <10%.
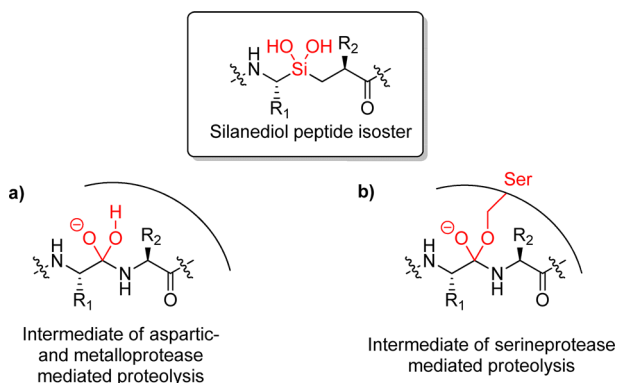

Figure 4. Simplified comparison of silanediol peptide isosters with intermediates of protolytic cleavage by (a) aspartic- and metalloproteases and (b) serine proteases.

0.94 (m, 15H). ^{13}C NMR (100 MHz, CDCl₃) δ (ppm) 174.9, 173.9, 171.8, 133.7, 132.7, 132.1, 128.8, 128.2, 127.82, 127.77, 127.1, 126.5, 126.2, 55.7, 43.7, 39.7, 39.0, 38.3 (dd, J = 26.5 Hz, J = 21.2 Hz), 37.1, 31.7, 30.7, 25.9, 25.0, 23.7, 21.0, 20.2, 15.2, 13.9, 11.8 (t, J = 20.2 Hz), 11.1. ^{19}F NMR (377 MHz, CDCl₃) δ (ppm) −129.4, −135.8. HRMS

(silanediol was formed during ionization) C₃₀H₄₇N₃O₅Si [M + K⁺]; calculated, 596.2922; found, 596.2918.

N-((2S,3S)-1-(((R)-1-((3-(Butylamino)-3-oxopropyl)-difluorosilyl)-3-methylbutyl)amino)-3-methyl-1-oxo-pentan-2-yl)-2-naphthamide (11′). The compound was synthesized according to general procedure B from diphenylsilane **26** (0.03 mmol), affording the product (11.8 mg, 72%) as a colorless solid. ^{1}H NMR (400 MHz, CDCl₃) δ (ppm) 8.36 (s, 1H), 7.84−7.95 (m, 4H), 7.70 (bs, 1H), 7.56 (dquin, 2H, J = 7.0 Hz, J = 1.4 Hz), 7.22−7.26 (m, 1H), 5.68 (bs, 1H), 4.70 (t, 1H, J = 8.2 Hz), 3.17 (dd, 2H, J = 13.0 Hz, J = 7.0 Hz), 2.90−2.97 (m, 1H), 2.30−2.40 (m, 2H), 2.03−2.14 (m, 1H), 1.20−1.72 (m, 9H), 1.07−1.15 (m, 2H), 1.02 (d, 3H, J = 6.8 Hz), 0.96 (t, 3H, J = 7.3 Hz), 0.84−0.92 (m, 9H). ^{13}C NMR (100 MHz, CDCl₃) δ (ppm) 174.8, 173.9, 168.2, 135.1, 132.7, 130.8, 129.2, 128.7, 128.1, 128.0, 127.9, 127.0, 123.7, 39.8, 39.2, 38.7 (dd, J = 24.8 Hz, J = 21.8 Hz), 37.3, 31.7, 30.6, 26.0, 25.4, 23.7, 22.8, 21.1, 20.1, 15.6, 13.8, 11.6 (t, J = 19.9 Hz), 11.3. ^{19}F NMR (377 MHz, CDCl₃) δ (ppm) −131.6, −135.6. HRMS (silanediol was formed during ionization) C₂₉H₄₅N₃O₅Si [M + Na⁺]; calculated, 566.3026; found, 566.3005.

(2S,3S)-N-((R)-1-((3-(Butylamino)-3-oxopropyl)-difluorosilyl)-3-methylbutyl)-3-methyl-2-(2-phenylacetamido)pentanamide (12′). The compound was synthesized according to general procedure B from diphenylsilane **27** (0.03 mmol), affording the product (13.8 mg, 100%) as a light brown solid. ^{1}H NMR (400 MHz, CDCl₃) δ (ppm) 8.02 (bs, 1H), 7.37−7.24 (m, 5H), 6.46 (d, 1H, J = 8.8 Hz), 5.73 (t, 1H, J = 5.6 Hz), 4.46 (t, 1H, J = 8.0 Hz), 3.60 (AB system, 2H, J = 15.6 Hz), 3.23 (dt, 2H, J = 7.2 Hz, J = 6.0 Hz), 2.73−2.80 (m, 1H), 2.23−2.36 (ddd, 2H, J = 15.6 Hz, J = 12.4 Hz, J = 7.6 Hz), 1.72−1.82 (m, 1H), 1.57−1.68 (m, 1H), 1.28−1.55 (m, 8H), 0.95−1.06 (m, 2H), 0.78−0.94 (m, 15H). ^{13}C NMR (100 MHz, CDCl₃) δ (ppm) 174.9, 173.7, 171.9, 134.5, 129.3(2C), 129.2(2C), 127.7, 55.8, 43.6, 39.7, 39.0, 38.4 (dd, J = 26.4 Hz, J = 20.6 Hz), 36.9, 31.8, 30.7, 26.0, 25.0, 23.7, 21.1, 20.0, 15.3, 13.9, 11.8 (dd, J = 21.1 Hz, J = 19.0 Hz), 11.1. ^{19}F NMR (377 MHz, CDCl₃) δ (ppm) −130.1, −136.8. HRMS (silanediol was formed during ionization) C₂₆H₄₅N₃O₅Si [M+K⁺]; calculated, 546.2766; found, 546.2887.

(2S,3S)-2-Acetamido-N-((R)-1-((3-(butylamino)-3-oxo-propyl)difluorosilyl)-3-methylbutyl)-3-methylpentanamide (13′). The compound was synthesized according to general procedure B from diphenylsilane **28** (0.030 mmol), affording the product (11.8 mg, 100%) as a light brown solid. ^{1}H NMR (400 MHz, CDCl₃) δ (ppm) 8.48 (bs, 1H), 6.83 (d, 1H, J = 9.2 Hz), 5.73 (t, 1H, J = 6.0 Hz), 4.58 (t, 1H, J = 8.8 Hz), 3.24 (dt, 2H, J = 6.8 Hz, J = 6.0 Hz),
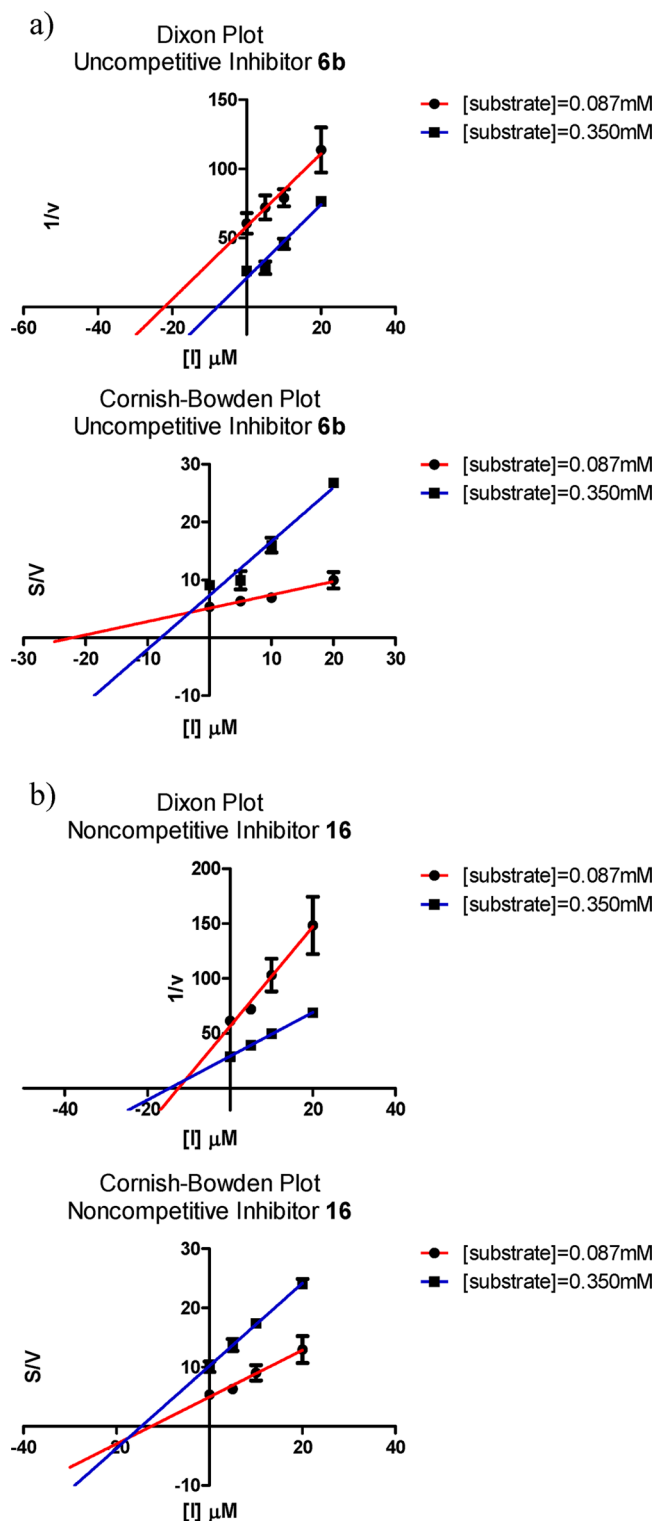
a)

Dixon Plot
Uncompetitive Inhibitor 6b

[substrate]=0.087mM
[substrate]=0.350mM

Cornish-Bowden Plot
Uncompetitive Inhibitor 6b

[substrate]=0.087mM
[substrate]=0.350mM

b)

Dixon Plot
Noncompetitive Inhibitor 16

[substrate]=0.087mM
[substrate]=0.350mM

Cornish-Bowden Plot
Noncompetitive Inhibitor 16

[substrate]=0.087mM
[substrate]=0.350mM

Figure 5. Representative Dixon and Cornish−Bowden plots. (a) Uncompetitive inhibitors, **6b**, **11**, and **12**. (b) Noncompetitive inhibitors **16** and **17**.

2.75−2.80 (m, 1H), 2.23−2.40 (m, 2H), 2.05 (s, 3H), 1.76−1.84 (m, 1H), 1.64−1.73 (m, 1H), 1.30−1.58 (m, 6H), 1.04−1.14 (m, 4H), 0.83−0.97 (m, 15H). ^{13}C NMR (100 MHz, CDCl$_3$) δ (ppm) 174.9, 173.7, 170.8, 55.5, 47.1, 39.6, 38.3 (dd, J = 27.2 Hz, J = 20.1 Hz), 37.1, 31.5, 29.7, 25.8, 25.0, 23.6, 23.0, 20.9, 20.0, 15.1, 13.7, 11.8 (dd, J = 22.7 Hz, J = 18.5 Hz), 11.1. ^{19}F NMR (377 MHz, CDCl$_3$) δ (ppm)

Table 2. Selectivity Data of Selected Inhibitors[a] toward Human Neutrophile Elastase, Trypsin, Chymotrypsin, Porcine Pancreatic Elastase, Cathepsin G, Plasmin, and Thrombin

	IC$_{50}$ (μM)					
	6b	**11**	**12**	**16**	**17**	AEBSF
HNE	18	16	38	14	14	130
trypsin	NI[b]	NI[b]	NI[b]	58	89	10
chymotrypsin	NI[b]	NI[b]	NI[b]	110	150	12
PPE	NI[b]	NI[b]	NI[b]	NI[b]	55	160
cathepsin G	NI[b]	NI[b]	NI[b]	120	NI[b]	250
plasmin	NI[b]	NI[b]	NI[b]	NI[b]	99	240
thrombin	NI[b]	NI[b]	NI[b]	92	100	62

[a]The IC$_{50}$ values are the average of at least two determinations with a standard deviation <10%. [b]NI: No inhibition observed at 100 μM. HNE, human neutrophil elastase; PPE, porcine pancreatic elastase; AEBSF, 4-(2-aminoethyl) benzenesulfonyl fluoride hydrochloride.

−128.7, −137.2. HRMS (silanediol was formed during ionization) C$_{20}$H$_{41}$N$_3$O$_5$Si [M + K$^+$]; calculated, 470.2453; found, 470.2470.

(2S,3S)-N-((R)-1-((3-(Butylamino)-3-oxopropyl)-difluorosilyl)-3-methylbutyl)-3-methyl-2-(2,2,2-trifluoroacetamido)-pentanamide (14′). The compound was synthesized according to general procedure B from diphenylsilane **29** (0.04 mmol) affording the product (13.4 mg, 69%) as a colorless solid. ^{1}H NMR (400 MHz, CDCl$_3$) δ (ppm) 7.47 (bd, 1H, J = 8.3 Hz), 6.95 (bd, 1H, J = 5.8 Hz), 5.83 (bt, 1H, J = 5.4 Hz), 5.88 (dd, 1H, J = 8.3 Hz, J = 7.0 Hz), 3.23−3.31 (m, 2H), 2.42 (dt, 2H, J = 7.6 Hz, J = 4.7 Hz), 1.88−1.96 (m, 1H), 1.44−1.54 (m, 6H), 1.30−1.38 (m, 4H), 1.12−1.22 (m, 2H), 0.84−0.96 (m, 15H). ^{13}C NMR (100 MHz, CDCl$_3$) δ (ppm) 175.5, 170.6, 157.3 (q, J = 37.5 Hz), 115.9 (q, J = 285.4 Hz), 57.2, 40.3, 39.7 (dd, J = 11.5 Hz, J = 7.9 Hz), 39.3, 37.8, 31.5, 29.8, 25.7, 25.0, 23.6, 21.3, 20.1, 15.2, 13.8, 11.3, 9.7 (t, J = 18.7 Hz). ^{19}F NMR (377 MHz, CDCl$_3$) δ (ppm) −75.6, −134.3, −135.7. HRMS (silanediol was formed during ionization) C$_{20}$H$_{38}$F$_3$N$_3$O$_5$Si [M + Na$^+$]; calculated, 508.2431; found, 508.2413.

(2S,3S)-N-((R)-1-(Difluoro(methyl)silyl)-3-methylbutyl)-3-methyl-2-(2-(naphthalen-2-yl)acetamido)pentanamide (15′). The compound was synthesized according to a modified literature procedure.[24] To a solution of di-p-tolyl silane **35** (20.5 mg, 0.03 mmol) in CH$_2$Cl$_2$ (0.2 mL) was added TFA (0.2 mL), and the reaction was stirred for 36 h. The reaction was cooled to 0 °C, and ammonium hydroxide (25%w/w, 0.2 mL, 1.35 mmol) was added. The reaction was stirred for 1 h at 0 °C after which hydrofluoric acid (48% in H$_2$O, 0.175 mL, 4.94 mmol) was added, and the reaction was stirred for further 30 min. CH$_2$Cl$_2$ was added, and the reaction was washed with H$_2$O and brine, dried over Na$_2$SO$_4$ and evaporated in vacuo, affording the product, (15.6 mg, 100%) as a colorless solid. ^{1}H NMR (400 MHz, CDCl$_3$) δ (ppm) 7.80−7.85 (m, 2H), 7.69 (bs, 1H), 7.56−7.62 (m, 1H), 7.46−7.52 (m, 2H), 7.32 (dd, 2H, J = 8.4 Hz, J = 1.8 Hz), 6.02 (bd, 1H, J = 8.8 Hz), 4.44 (t, 1H, J = 8.6 Hz), 3.73 (s, 2H), 2.64 (dq, 1H, J = 11.3 Hz, J = 3.4 Hz), 1.45−1.55 (m, 3H), 1.30−1.40 (m, 3H), 0.70−0.90 (m, 12H), 0.07 (s, 3H). ^{19}F NMR (377 MHz, CDCl$_3$) δ (ppm) −130.1, −132.0. HRMS (silanediol was formed during ionization) C$_{24}$H$_{36}$N$_2$O$_4$Si [M + Na$^+$]; calculated, 467.2325; found, 467.2342.

(2S,3S)-N-((R)-1-((3-(Butylamino)-3-oxopropyl)diphenylsilyl)-3-methylbutyl)-3-methyl-2-(2-(naphthalen-2-yl)acetamido)-pentanamide (16). The compound was synthesized according to a literature procedure.[23] ^{1}H NMR (400 MHz, CDCl$_3$) δ (ppm) 7.73−7.84 (m, 3H), 7.59 (s, 1H), 7.52−7.56 (m, 2H), 7.34−7.50 (m, 10H), 7.20 (dd, 1H, J = 8.3 Hz, J = 1.6 Hz), 5.84 (d, 1H, J = 9.0 Hz), 5.74 (bs, 1H), 5.56 (d, 1H, J = 10.2 Hz), 4.37 (td, 1H, J = 11.3 Hz, J = 3.2 Hz), 4.12 (dd, 1H, J = 8.8 Hz, J = 6.9 Hz), 3.69 (dd, 2H, J = 21.5 Hz, J = 15.8 Hz), 3.15 (dd, 2H, J = 13.0 Hz, J = 6.9 Hz), 2.30 (ddd, 1H, J = 14.4 Hz, J = 11.8 Hz, J = 4.7 Hz), 2.02 (ddd, 1H, J = 14.5 Hz, J = 11.6 Hz, J = 5.9 Hz), 1.70−1.80 (m, 1H), 1.15−1.48 (m, 10H), 0.88 (t, 3H,

J = 7.3 Hz), 0.83 (d, 3H, J = 6.0 Hz), 0.74−0.82 (m, 1H), 0.68−0.74 (m, 9H). ^{13}C NMR (100 MHz, CDCl$_3$) δ (ppm) 174.1, 170.9, 170.4, 135.7 (2C), 135.4 (2C), 133.7, 132.6, 132.3, 132.2, 132.1, 130.24, 130.15, 129.0, 128.35 (2C), 128.31 (2C), 128.2, 127.8, 127.7, 127.0, 126.6, 126.2, 58.4, 44.0, 40.2, 39.4, 36.5, 34.9, 31.8, 30.7, 25.1, 24.7, 23.6, 21.1, 20.2, 15.6, 13.9, 11.3, 7.8. HRMS C$_{42}$H$_{55}$N$_3$O$_3$Si [M + Na$^+$]; calculated, 700.3910; found, 700.3952.

(S)-N-(2-(Butylamino)-2-oxoethyl)-4-methyl-2-((2S,3S)-3-methyl-2-(2-(naphthalen-2-yl)acetamido)pentanamido)-pentanamide (17). The compound was synthesized according to general procedure A from carbamate **39** (0.35 mmol) and 2-naphthaleneacetic acid (0.70 mmol). The crude compound was purified by FC (eluent: 3% MeOH in CH$_2$Cl$_2$) affording the product (114.7 mg, 63%) as a colorless solid. ^{1}H NMR (400 MHz, CDCl$_3$) δ (ppm) 8.55−8.72 (m, 2H), 8.15 (bs, 1H), 7.66−7.78 (m, 4H), 7.60 (bs, 1H), 736−7.43 (m, 3H), 5.00−5.12 (m, 1H), 4.89 (t, 1H, J = 8.5 Hz), 4.56−4.67 (m, 1H), 3.85 (d, 1H, J = 14.6 Hz), 3.78 (d, 1H, J = 14.6 Hz), 3.64 (d, 1H, J = 13.9 Hz), 2.97 (non, 2H, J = 6.8 Hz), 1.62−1.75 (m, 2H), 1.44−1.60 (m, 3H), 1.12−1.22 (m, 2H), 0.94−1.10 (m, 3H), 0.84−0.92 (m, 6H), 0.74−0.82 (m, 6H), 0.69 (t, 3H, J = 7.3 Hz). ^{13}C NMR (100 MHz, CDCl$_3$) δ (ppm) 172.5, 171.4, 171.0, 169.2, 134.0, 133.6, 132.4, 127.94, 127.86, 127.7, 127.63, 127.59, 126.0, 125.6, 57.3, 51.3, 43.2, 43.1, 43.0, 39.3, 31.5, 25.5, 25.1, 23.7, 22.5, 20.0(2C), 15.4, 13.7, 11.7. HRMS C$_{30}$H$_{44}$N$_4$O$_4$ [M + Na$^+$]; calculated, 547.3260; found, 547.3265.

(S)-N-(2-(Butylamino)-2-oxoethyl)-4-methyl-2-((2S,3S)-3-methyl-2-(2-phenylacetamido)-pentanamido)pentanamide (18). The compound was synthesized according to general procedure A from carbamate **39** (0.16 mmol) and phenylacetic acid (0.32 mmol). The crude compound was purified by FC (eluent: 2−5% MeOH in CH$_2$Cl$_2$) affording the product (32.5 mg, 43%) as a colorless solid. ^{1}H NMR (400 MHz, CDCl$_3$) δ (ppm) 7.99−8.10 (m, 2H), 7.42 (bs, 1H), 7.35 (bs, 1H), 7.21−7.32 (m, 5H), 4.82 (q, 1H, J = 7.4 Hz), 4.69 (t, 1H, J = 8.2 Hz), 4.39 (dd, 1H, J = 16.3 Hz, J = 7.0 Hz), 3.74 (dd, 1H, J = 16.1 Hz, J = 4.0 Hz), 3.66 (d, 1H, J = 14.8 Hz), 3.62 (d, 1H, J = 14.8 Hz), 3.03−3.17 (m, 2H), 1.64−1.73 (m, 2H), 1.40−1.62 (m, 3H), 1.31−1.39 (m, 2H), 1.19−1.29 (m, 2H), 0.92−1.03 (m, 1H), 0.90 (d, 3H, J = 6.4 Hz), 0.88 (d, 3H, J = 6.4 Hz), 0.84 (t, 3H, J = 7.3 Hz), 0.75−0.81 (m, 6H). ^{13}C NMR (100 MHz, CDCl$_3$) δ (ppm) 172.4, 171.5, 171.2, 169.1, 135.9, 129.4(2C), 128.6(2C), 126.9, 57.5, 51.6, 43.2, 43.1, 42.7, 39.4, 38.7, 31.6, 25.1, 25.0, 23.2, 22.6, 20.2, 15.4, 13.9, 11.6. HRMS C$_{26}$H$_{42}$N$_4$O$_4$ [M+Na$^+$]; calculated, 497.3104; found, 497.3089.

(2S,3S)-2-Acetamido-N-((S)-1-((2-(butylamino)-2-oxo-ethyl)-amino)-4-methyl-1-oxopentan-2-yl)-3-methylpentanamide (19). The compound was synthesized according to general procedure A from carbamate **39** (0.23 mmol) and acetic acid (0.46 mmol). The crude compound was purified by FC (eluent: 2−4% MeOH in CH$_2$Cl$_2$) affording the product (27.3 mg, 30%) as a colorless solid. ^{1}H NMR (400 MHz, CD$_3$OD) δ (ppm) 8.25−8.33 (m, 2H), 8.10 (d, 1H, J = 7.4 Hz), 7.79 (t, 1H, J = 4.6 Hz), 4.23−4.29 (m, 1H), 4.12−4.17 (m, 1H), 3.90−3.97 (m, 1H), 3.66−3.72 (m, 1H), 3.19−3.23 (m, 2H), 1.99 (s, 3H), 1.46−1.74 (m, 5H), 1.15−1.40 (m, 5H), 0.89−0.98 (m, 15H). ^{13}C NMR (100 MHz, CDCl$_3$) δ (ppm) 175.1, 174.4, 173.8, 171.3, 59.6, 53.9, 43.5, 41.0, 40.2, 37.8, 32.5, 26.1, 25.8, 23.3, 22.4, 22.0, 21.0, 15.9, 14.1, 11.3. HRMS C$_{20}$H$_{38}$N$_4$O$_4$ [M + Na$^+$]; calculated, 421.2791; found, 421.2782.

(S)-N-(2-(Butylamino)-2-oxoethyl)-4-methyl-2-((2S,3S)-3-methyl-2-(2,2,2-trifluoroacet-amido)pentanamido)-pentanamide (20). The compound was synthesized according to general procedure A from carbamate **39** (0.16 mmol) and trifluoro-acetic acid (0.32 mmol). The crude compound was purified by FC (eluent: 2−4% MeOH in CH$_2$Cl$_2$) affording the product (3.0 mg, 4%) as a colorless solid. ^{1}H NMR (400 MHz, CDCl$_3$) δ (ppm) 7.80 (d, 1H, J = 8.6 Hz), 7.74 (d, 1H, J = 7.1 Hz), 7.48 (bs, 1H), 6.62 (t, 1H, J = 5.8 Hz), 4.74 (q, 1H, J = 7.8 Hz), 4.65 (t, 1H, J = 8.4 Hz), 4.18 (dd, 1H, J = 16.5 Hz, J = 6.0 Hz), 3.91 (dd, 1H, J = 16.6 Hz, J = 4.5 Hz), 3.17−3.31 (m, 2H), 1.81−1.90 (m, 1H), 1.44−1.69 (m, 5H), 1.29−1.39 (m, 3H), 1.05−1.17 (m, 1H), 0.85−0.98 (m, 15H). ^{13}C NMR (100 MHz, CDCl$_3$) δ (ppm) 172.3, 169.8, 168.3, 157.4 (q, J = 37.2 Hz), 116.0 (q, J = 285.3 Hz), 58.1, 51.9, 43.1, 42.8, 39.4, 38.1, 31.4,

25.02, 24.96, 22.8, 22.6, 20.1, 15.3, 13.8, 11.3. ^{19}F NMR (377 MHz, CDCl$_3$) δ (ppm) −75.6 (d, J = 27.0 Hz). HRMS C$_{20}$H$_{35}$F$_3$N$_4$O$_4$ [M + Na$^+$]; calculated, 475.2508; found, 475.2487.

Biology. HNE and cathepsin G were purchased from Biocentrum Ltd. Trypsin, chymotrypsin, and porcine pancreatic elastase were purchased from Sigma-Aldrich. Thrombin and plasminogen were purified as described previously.[29] Chromogenic substrates were purchased from Sigma-Aldrich, except for H-D-Pro-L-Phe-L-Arg-p-nitroanilide, which was purchased from Chromogenix. Hydrolysis was monitored with a FLUOstar Omega platereader, kinetic mode, wavelength 405 nm. Reactions were performed in 96-well microtiter plates. All data points were collected in duplicates. The applied assay buffer was 0.1 M HEPES buffer containing 0.5 M NaCl at pH 7.25.

Human Neutrophil Elastase: IC$_{50}$ Determination. The inhibitor stock solutions (100 mM in DMSO) were further diluted at 7 different concentrations (5−500 μM) in assay buffer. HNE (2.8 μM in 0.05 M sodium acetate buffer containing 0.5 M NaCl, pH 5.5) was diluted immediately prior to use in assay buffer to a concentration of 300 nM. The chromogenic substrate (N-succinyl-Ala-Ala-Pro-Val-p-nitroanilide) stock solution (70 mM) in DMSO was diluted immediately prior to use in assay buffer to a concentration of 3.5 mM. Assays were run in dublicates in a 96-well plate in a total volume of 200 μL. DMSO was kept at 5.5% in every well. Enzyme (20 μL, final enzyme concentration 30 nM) and inhibitor solutions (20 μL, final inhibitor concentrations 0.5−50 μM) were incubated in assay buffer for 2 h at 25 °C. Chromogenic substrate (20 μL, final substrate concentration 0.35 mM) was added to the wells, and the rate of hydrolysis was determined by monitoring the absorbance at 405 nm at 25 °C for 20 min. The rate of hydrolysis (ΔA/min) was linear between 5 and 15 min of reaction.

K$_i$ Determination: Dixon Plot and Cornish−Bowden Plot. The mechanism of inhibition was studied by performing Dixon and Cornish−Bowden plots.[26,27] The inhibitory potency was measured at two substrate concentrations, 0.0875 mM and 0.35 mM.

The inhibitor stock solutions (100 mM in DMSO) were further diluted at 3 different concentrations (50−200 μM) in assay buffer. Human neutrophil elastase (2.8 μM in 0.05 M sodium acetate buffer containing 0.5 M NaCl, pH 5.5) was diluted immediately prior to use in assay buffer to a concentration of 300 nM. The chromogenic substrate (N-succinyl-Ala-Ala-Pro-Val-p-nitroanilide) stock solution 70 mM in DMSO was diluted immediately prior to use in assay buffer at two different concentrations of 0.875 mM and 3.5 mM. Assays were run in duplicates in a total volume of 200 μL. DMSO was kept at 5.5% in every well. Enzyme (20 μL, final enzyme concentration 30 nM) and inhibitor solutions (20 μL, final inhibitor concentrations 5−20 μM) were incubated in assay buffer for 2 h at 25 °C. Chromogenic substrate (20 μL, final substrate concentrations 0.0875 mM or 0.35 mM) was added to the wells, and the rate of hydrolysis was determined by monitoring the absorbance at 405 nm at 25 °C for 20 min.

■ ASSOCIATED CONTENT

Ⓢ Supporting Information

Experimental data and spectroscopic data, experimental and spectroscopic data for the conversion of difluorosilanes to silanediols at assay conditions, dose−response curves, Dixon plots, and Cornish−Bowden plots. This material is available free of charge via the Internet at http://pubs.acs.org.

■ AUTHOR INFORMATION

Corresponding Author

*(J.J.E.) Phone: +45 87155449. E-mail: jje@mb.au.dk. (T.S.) Phone: +45 87155968. E-mail: ts@chem.au.dk.

Author Contributions

J.L.H.M. performed the syntheses and enzyme kinetics studies; T.L.A. performed part of the syntheses; S.S. and H.N. assisted in the interpretation of the enzyme kinetics data; J.J.E. and T.S. supervised the project.

ABBREVIATIONS USED

AEBSF, 4-(2-aminoethyl)benzenesulfonyl fluoride hydrochloride; Boc, *tert*-butyloxycarbonyl; COPD, chronic obstructive pulmonary disease; DMSO, dimethyl sulfoxide; EDC, *N*-ethyl-*N'*-(3-dimethylamino-propyl)carbodiimide hydrochloride; FC, flash chromatography; HNE, human neutrophil elastase; HOBt, 1-hydroxybenzotriazole; HXMS, hydrogen exchange mass spectrometry; MD, molecular dynamics; PPE, porcine pancreatic elastase; TFA, trifluoroacetic acid; THF, tetrahydrofuran; THP, tetrahydropyranyl

REFERENCES

(1) Janoff, A.; Scherer, J. Mediators of Inflammation in leukocyte lysosomes, IX. Elastinolytic activity in granules of human poly-morphonuclear leukocytes. *J. Exp. Med.* **1968**, *128*, 1137−1155.

(2) Baggiolini, M.; Schnyder, J.; Bretz, U.; Dewald, B.; Ruch, W. Cellular mechanisms of proteinase released from inflammatory cells and the degradation of extracellular proteins. *Ciba Found. Symp.* **1979**, *75*, 105−121.

(3) Korkmaz, B.; Moreau, T.; Gauthier, F. Neutrophil elastase, proteinase 3 and cathepsin G: Physicochemical properties, activity and physiopathological functions. *Biochimie* **2008**, *90*, 227−242.

(4) Djekic, U. V.; Gaggar, A.; Weathington, N. M. Attacking the multi-tiered proteolytic pathology of COPD: New insights from basic and translational studies. *Pharmacol. Ther.* **2009**, *121*, 132−146.

(5) Wang, Z.; Chen, F.; Zhai, R.; Zhang, L.; Su, L.; Lin, X.; Thompson, T.; Christiani, D. C. Plasma neutrophil elastase and elafin imbalance is associated with acute respiratory distress syndrome (ARDS) development. *PLoS one* **2009**, *4*, 1−10.

(6) Kawabata, K.; Hagio, T.; Matsuoka, S. The role of neutrophil elastase in acute lung injury. *Eur. J. Pharmacol.* **2002**, *451*, 1−10.

(7) Voynow, J. A.; Fischer, B. M.; Zheng, S. Proteases and cystic fibrosis. *Int. J. Biochem. Cell Biol.* **2008**, *40*, 1238−1245.

(8) Shapiro, S. D.; Goldstein, N. M.; Houghton, A. M.; Kobayashi, D. K.; Kelley, D.; Belaaouaj, A. Neutrophil elastase contributes to cigarette smoke-induced emphysema in mice. *Am. J. Pathol.* **2003**, *163*, 2329−2335.

(9) Churg, A.; Wang, R. D.; Xie, C.; Wright, J. L. α-1-Antitrypsin ameliorates cigarette smoke-induced emphysema in the mouse. *Am. J. Respir. Crit. Care Med.* **2003**, *168*, 199−207.

(10) Groutas, W. C.; Dou, D.; Alliston, K. R. Neutrophil elastase inhibitors. *Expert Opin. Ther. Patents* **2011**, *21*, 339−354.

(11) Lucas, S. D.; Costa, E.; Guedes, R. C.; Moreira, R. Targetting COPD: advances on low-molecular-weight inhibitors of human neutrophil elastase. *Med. Res. Rev.* **2011**, DOI: 10.1002/med.20247.

(12) Inoue, Y.; Omodani, T.; Shiratake, R.; Okazaki, H.; Kuromiya, A.; Kubo, T.; Sato, F. Development of a highly water-soluble peptide-based human neutrophil elastase inhibitor; AE-3763 for treatment of acute organ injury. *Bioorg. Med. Chem.* **2009**, *17*, 7477−7486.

(13) Kawabata, K.; Suzuki, M.; Sugitani, M.; Imaki, K.; Toda, M. Miyamoto, T. ONO-5046, a novel inhibitor of human neutrophil elastase. *Biochem. Biophys. Res. Commun.* **1991**, *177*, 814−820.

(14) Hsieh, P.-W.; Yu, H.-P.; Chang, Y.-J.; Hwang, T.-L. Synthesis and evaluation of benzoxazinone derivatives on activity of human neutrophil elastase and on hemorrhagic shock-induced lung injury in rats. *Eur. J. Med. Chem.* **2010**, *45*, 3111−3115.

(15) http://www.ono.co.jp/eng/cn/contents/sm_cn_052703.pdf (accessed July 2012).

(16) Ohbayashi, H. Current synthetic inhibitors of human neutrophil elastase in 2005. *Expert Opin. Ther. Patents* **2005**, *15*, 759−771.

(17) Kim, J.; Hewitt, G.; Carroll, P.; Sieburth, S. McN. Silanediol Inhibitors of Angiotensin-Converting Enzyme. Synthesis and Evaluation of Four Diastereomers of Phe[Si]Ala Dipeptide Analogues. *J. Org. Chem.* **2005**, *70*, 5781−5789.

(18) Chen, C.-A.; Sieburth, S. M. N.; Glekas, A.; Hewitt, G. W.; Trainor, G. L.; Erickson-Viitanen, S.; Garber, S. S.; Cordova, B.; Jeffry, S.; Klabe, R. M. Drug design with a new transition state analog of the hydrated carbonyl: silicon-based inhibitors of the HIV protease. *Chem. Biol.* **2001**, *8*, 1161−1166.

(19) Mills, J. S.; Showell, G. A. Exploitation of silicon medicinal chemistry in drug discovery. *Expert Opin. Invest. Drugs* **2004**, *13*, 1149−1157.

(20) Showell, G. A.; Montana, J. G.; Chadwick, J. A.; Higgs, C.; Hunt, H. J.; MacKenzie, R. E.; Price, S.; Wilkinson, T. J. Silicon Diols, Effective Inhibitors of Human Leukocyte Elastase. *Organosilicon Chemistry VI: From Molecules to Materials*; John Wiley & Sons: New York, 2005; pp 569−574.

(21) Nielsen, L.; Lindsay, K. B.; Faber, J.; Nielsen, N. C.; Skrydstrup, T. Stereocontrolled synthesis of methyl silanediol peptide mimics. *J. Org. Chem.* **2007**, *72*, 10035−10044.

(22) Nielsen, L.; Skrydstrup, T. Sequential C-Si bond formations from diphenylsilane: application to silanediol peptide isostere precursors. *J. Am. Chem. Soc.* **2008**, *130*, 13145−13151.

(23) Hernández, D.; Lindsay, K. B.; Nielsen, L.; Mittag, T.; Bjerglund, K.; Friis, S.; Mose, R.; Skrydstrup, T. Further studies towards the stereocontrolled synthesis of silicon-containing peptide mimics. *J. Org. Chem.* **2010**, *75*, 3283−3293.

(24) Hernández, D.; Mose, R.; Skrydstrup, T. Reductive lithiation of methyl substituted diarylmethylsilanes: application to silanediol peptide precursors. *Org. Lett.* **2011**, *13*, 732−735.

(25) See Supporting Information for further descriptions of NMR studies confirming the conversion of difluorosilane to silanediol under the assay conditions.

(26) Dixon, M. The determination of enzyme inhibitor constants. *Biochem. J.* **1953**, *55*, 170−171.

(27) Cornish−Bowden, A. A simple graphical method for determining the inhibition constants of mixed, uncompetitive and non-competitive inhibitors. *Biochem. J.* **1974**, *137*, 143−144.

(28) Gottlieb, H. E.; Kotlyar, V.; Nudelman, A. NMR chemical shifts of common laboratory solvents as trace impurities. *J. Org. Chem.* **1997**, *62*, 7512−7515.

(29) Plasminogen: Deutsh, D. G.; Mertz, E. T. Plasminogen: purification from human plasma by affinity chromatography. *Science* **1970**, *170*, 1095−1096. Thrombin: Ngai, P. K.; Chang, J.-Y. A novel one-step purification of human alpha-thrombin after direct activation of crude prothrombin enriched from plasma. *Biochem. J.* **1991**, *280*, 805−808.